JOURNAL OF MATERIAL SCIENCE 33 (1998) 3065–3071

^{1}H nuclear magnetic resonance characterization of Portland cement: molecular diffusion of water studied by spin relaxation and relaxation time-weighted imaging

PU SEN WANG, M. M. FERGUSON*, G. ENG*, D. P. BENTZ, C. F. FERRARIS, J. R. CLIFTON
National Institute of Standards and Technology, Gaithersburg, MD 20899, USA
E-mail: pu.wang@nist.gov

Water molecular dynamics in a hardened Portland cement were characterized by proton Fourier transform nuclear magnetic resonance (NMR) at 400 MHz. Three different types of water molecule (physically bound, chemically bound and porous trapped) were observed. When the hardened cement sample was heated at 105 °C, the physically bound water diffused out of the sample as a function of the heating time while the chemically bound water remained in a stable form. A trace amount of the porously trapped water was also detected to remain in the cavities of the hardened cement even after heating for up to 20 h at this temperature. The loss of the physically bound water proved to be a diffusion-controlled process as evidenced from the NMR data and from a gravimetric technique. A Pake doublet was observed in the NMR spectra. This is a result of the oscillation of the water molecules with hindered molecular motions due to their entrapment in the cement pores. Soaking the dried samples in water resulted in the diffusion of water back into the hardened cement as physically bound water. Nuclear spin–spin relaxation time, T_2-weighted imaging showed that the distribution of the physically bound water inside the cylindrical sample formed a doughnut shape after overnight soaking. The residual air in the cement pores may have slowed down the diffusion rate of the water molecules back into the dried cement.

1. Introduction

Cement is one of the most commonly used building materials and has a complex composition. Its hydration mechanism has been an interesting subject and numerous efforts have been made to understand it [1, 2]. The state of water in a hydrating cement paste directly influences the mechanical and transport properties of this composite material, as well as their evolution with time, and directly impacts the durability of concrete structures [3, 4]. Thus, understanding the state of the water in a cement paste sample is critical from both a scientific and a technological standpoint.

At least three types of water can be distinguished in a hydrating cement paste. Chemically bound water is that water which is directly incorporated into the structure of the cement hydration products. Physically bound water is water that is strongly adsorbed on the surfaces of the cement particles and reaction products, which can easily have surface areas of the order of 100–1000 m^2g^{-1}. Bulk or "free" water is water which is contained in the capillary and gel pores of the hydrating cement paste. Another delineation of water often employed for cement paste is a division into evaporable and non-evaporable water (water removable by heating to 105 °C and 950–1050 °C, respectively [5]). A typical cement paste will contain 0.23 g non-evaporable water per gram of cement powder, when completely hydrated. It must be kept in mind, of course, that, if the water-to-cement ratio is low enough (less than about 0.4), complete hydration is not possible owing to a lack of available space for precipitation and growth of the hydration products.

Nuclear magnetic resonance (NMR) is a non-destructive technique which can provide a unique diagnosis of materials. NMR has the following advantages over other techniques in materials diagnosis.

(a) Samples can be characterized non-destructively for different nuclei at different frequencies for their spatial distribution.

(b) The sample can be characterized *in situ* in a number of ways, e.g. not only spin densities but also

*Visiting scientists from the Department of Chemistry, University of the District of Columbia, Washington DC 20008, USA.

different relaxation times can be measured to understand the environment of a specific nuclear spin.

(c) Any plane can be imaged without actually slicing the sample.

Since cement is a very complex multicomponent material, the chemical reactions and kinetics involved are also very complex. Magic angle spinning (MAS) NMR can provide some solutions to the problem of identification and structure of reaction products. Nuclear relaxation studies can also provide information on the chemical and physical states of the water molecules during hydration reactions as well as instant reaction kinetics. Modern NMR imaging techniques may shed some light on the material diffusion and internal distribution in a shaped cement sample during hydration. Regardless of what type of NMR experiment one utilizes in cement studies, ferrite components in the cement always impose a challenge to NMR technology.

Several studies have been published concerning NMR spectroscopy applications to cements [6–12]. Most of these investigations utililzed proton NMR to study the porosity and hydration of white cement pastes. White cements were used because they do not contain ferrites that cause large line broadening due to magnetic susceptibility. In other investigations,^{29}Si and^{27}Al MAS NMR spectroscopy was used to study the hydration products of a single component of cements, such as calcium oxide sulphoaluminate [13, 14]. Proton NMR imaging was also used to study water diffusion in hardenend cement pastes [7]. Again, white cement was used to increase the values of nuclear spin–spin relaxation time, T_2, and to avoid the artefact distortions of the picture due to the ferrite materials in the cement [15].

Our laboratory has published NMR imaging studies on the solid binder distribution in green ceramic bodies by either a stray-field imaging technique [16] or a gradient coils technique [17, 18]. We have also published a NMR imaging study of the powder distribution in a slurry by a "soft pulse" technique [19]. In the present study, proton NMR will be used to probe the nuclear spin–crystal lattice relaxation and nuclear spin–spin relaxation times of a hardened cement paste. Since the ferrite materials contained in the cement will result in extremely short T_2 values, a "hard-pulse" technique was used to image the distribution of the "bound" water in the cement samples.

2. Experimental procedures

2.1. Preparation of cement samples

Portland cement labelled as Cement 116 by the Cement and Concrete Reference Laboratory (CCRL) of the National Institute of Standards and Technology was mixed with distilled water in water-to-cement mass ratios, w/c, of 0.30 ± 0.01, 0.40 ± 0.01 and 0.50 ± 0.01. The chemical fractions of Cement 116 are $0.606\,60 \pm 0.000\,01$, $0.132\,18 \pm 0.000\,01$, $0.109\,50 \pm 0.000\,01$, $0.060\,61 \pm 0.000\,01$ and $0.062\,58 \pm 0.000\,01$ for tricalcium silicate, dicalcium silicate, tricalcium aluminate, tetracalcium aluminoferrite and gypsum, respectively. The average particle diameter was $4.8 \pm 0.1\,\mu m$ and the surface area was $3645.5 \pm 0.1\,cm^2\,g^{-1}$. The pastes were shaped into cylindrical pellets by moulding them in Tygon tubings of 6 mm inside diameter. A typical pellet had a mass of 0.52–0.68 g and was about 10 mm high and 6 mm in diameter. The pelletized samples were stored in sealed bottles for hardening until the measurements were made.

2.2. Nuclear magnetic resonance spectrometer and imaging facility

The one-pulse experiments and nuclear spin–spin relaxation time, T_2, measurements were performed using a Bruker MSL-400 spectrometer with a 20 mm radio-frequency (r.f.) resonant coil in the imaging probe at $400.134\,000 \pm 0.000\,001$ MHZ. T_2 values were measured by use of a multiple-pulse sequence of $\pi/2$–τ–(π)–τ–echo–D_0 to generate the nuclear spin echo signals. In this sequence, $\pi/2$ is a 90° r.f. pulse that had a width of 31 μs in our experiments. The variable delay, τ, ranges from a few microseconds to a few seconds. D_0 (equal to 20 s in our experiments) is a long delay during which the nucleus returns to equilibrium by releasing excitation energy through the crystal lattice.

The NMR imaging facility consists of a Bruker MSL-400 system with a selective excitation unit, a micro-imaging probe, a gradient drive unit, a low-power (5 W) linear amplifier and other accessories. The pulse sequence used to acquire the echo signals, phase encoding and T_2 weighting for image construction is D_0–$\pi/2$–τ–D_{10}–D_7–π–D_7–D_{10}–AQ–D_0, where τ is also used for the phase encoding time, AQ is the echo acquisition time, D_{10} and D_7 are the delays for T_2 weighting and gradient coil stabilization, respectively, and D_0 is the delay time (20 s). The typical phase encoding time for this solid imaging sequence is 400 μs. A maximum field gradient of approximately $6 \times 10^{-3}\,T\,cm^{-1}$ was generated for phase encoding. The details for this experiment can be found elsewhere [18].

3. Results and discussion

Fig. 1, curve a, shows the one-pulse spectrum of the Cement 116 sample with a water-to-cement mass ratio of 0.5, 1 day after mixing. The linewidth $H_{1/2}$ at half-maximum intensity is $10\,210 \pm 5$ HZ. The majority of the water is physically adsorbed on the powder surfaces of the cement particles, which are randomly oriented, thus accounting for the broadness of the line. Another reason for the line broadening is the magnetic susceptibility of the ferrite material(s) in the cement. Weak splittings can be observed on the top and to the right of the broad peak. These are assigned to the protons from the $Ca(OH)_2$ and "free" water that is trapped in the cement paste pores, respectively. They are weak compared with the main signal because the NMR spectrum was recorded 1 day after mixing and the hydration reaction is far from complete. One of the main hydration products of cement is $Ca(OH)_2$ and the water used in its formation is referred to as "chemically bound" water. The "free" water is still in a liquid

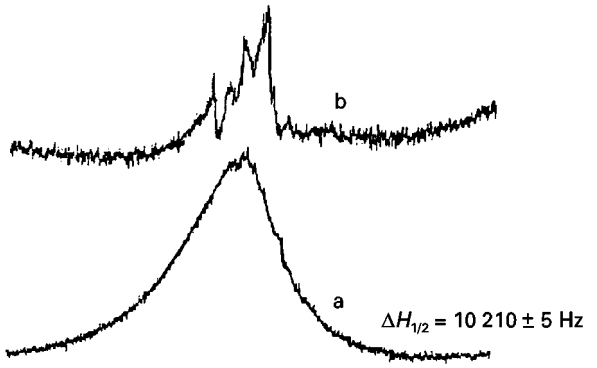

Figure 1 Single-pulse NMR spectrum of a $w/c = 0.5$ sample. Curve a, 1 day after mixing, showing the overwhelming physically bound water with a linewidth of 10 210 Hz at half-maximum intensity; curve b, after heating at 105 °C for 20 h, showing almost complete removal of physically bound water.

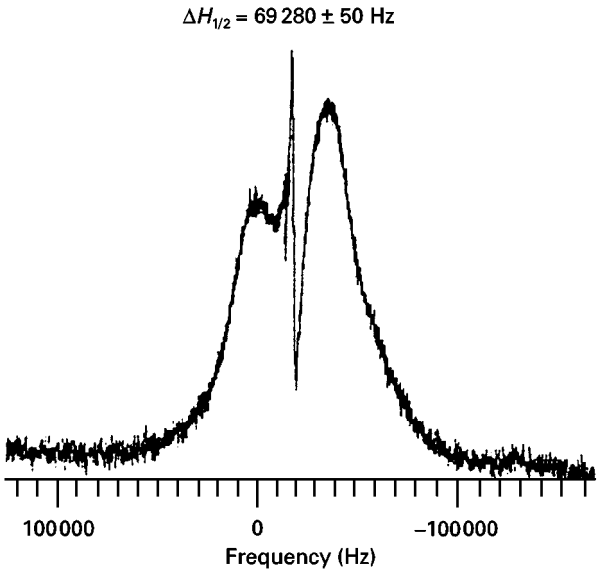

Figure 2 Proton NMR powder spectrum of a dry $Ca(OH)_2$ sample having a linewidth of 69 280 Hz. The — OH rotation narrowing can be clearly observed.

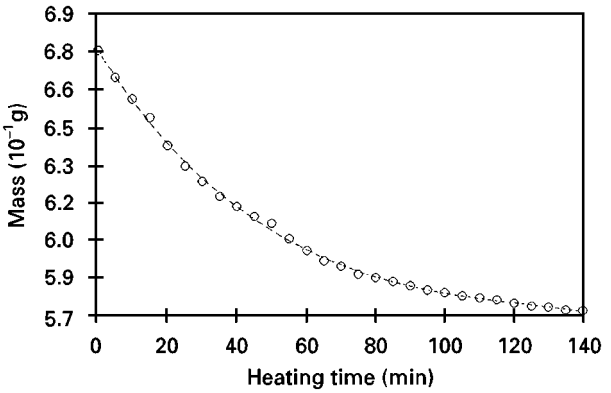

Figure 3 A plot of mass versus heating increments (105 °C; 5 min) for a $w/c = 0.4$ sample after setting for 33 days. The decay curve indicates a diffusion-controlled drying mechanism.

state and can tumble freely, thus accounting for its narrow linewidth. These phenomena can be seen more clearly when the sample was heated at 105 °C overnight (Fig. 1, curve b). Almost no physically bound water can be detected in the sample after heating at 105 °C overnight. Heating the sample may have accelerated the hydration reaction and converted some of the physically bound water to chemically bound water. Furthermore, it is interesting to observe that the "free" water trapped in the cement pores remains in the pores (right peak in Fig. 1b) even after heating overnight. The rest of the signal is due to the $Ca(OH)_2$ and the splitting and narrowing of the line width are due to –OH rotation [20–23].

The $Ca(OH)_2$ signal mentioned above is actually only part of the broad peak which is narrowed by the –OH rotation. Since $Ca(OH)_2$ is formed by the reaction of water with calcium oxide (CaO), the molecular motion for the water used in the reaction is the slowest of the three types of water. Hence its nuclear dipole–dipole interaction should be the largest which results in a large line broadening. Fig. 2 is a proton powder spectrum of pure $Ca(OH)_2$ dried at 105 °C overnight. The line width at half-maximum intensity is 69 280 ± 50 HZ. The hump to the right of the –OH narrowing is due to the anisotropic chemical shift, σ_1, along the X and Y axes. The crystal symmetry of $Ca(OH)_2$ is D_{3d} so that the X and Y axes are equivalent [22]. The hump to the left of the –OH narrowing is due to the anisotropic chemical shift,σ_1, along the Z axis. The right hump is more intense than the left hump since there is more spin density on the X–Y plane than along the Z axis.

After the sample with a water-to-cement mass ratio of 0.5 had set for several days, formation of a white layer was observed on the surface. NMR identification of this material proved it to be $Ca(OH)_2$. Consequently, it can be established that when the water content is high (as for a 0.5 mass ratio of water to cement), the hydration product, $Ca(OH)_2$, is carried out by the excess water from the bulk of the cement to the surface. This results in a heterogeneous sample with a shell rich in calcium hydroxide. Since water diffusivity in the calcium hydroxide is different from the rest of the cement sample, this shell will alter the water diffusion behaviour and results in a more complex drying mechanism.

A 0.4 water-to-cement mass ratio pellet (0.1930 g of water and 0.4825 g of cement) was used for incremental heating experiments after it had been allowed to set for 33 days after mixing. The increments of heating were 5 min intervals at 105 °C. The mass of the sample before heating was 0.6755 ± 0.0001 g. After 28 heating increments, a nearly constant mass of 0.5727 ± 0.0001 g was achieved. Fig. 3 shows the sample weight against the number of heating increments for the sample. The mass curve indicates a characteristic diffusion-controlled behaviour. A total loss of 0.1028 ± 0.0001 g of water was observed. Since the pellets were cast and sealed, no water was lost during setting. Thus, after setting at room temperature for 33 days, 0.1028 g of water remained as physically bound water and could be removed by heating, within 140 min. Conversely, 0.0902 g of water or 0.1869 g of water per gram of cement was chemically bound into

the hydration products. This corresponds to approximately 80% complete hydration, or two degrees of hydration (0.23 g of chemically bound water per 1 g of cement for complete hydration).

Fig. 4, curves a, b and c, shows the NMR spectra of this pellet before and after ten intervals of heating and after 20 intervals of heating (5 min each), respectively. Comparison of these spectra indicate that the physically bound water can be removed by heating at 105 °C. Using the signal height of σ_1 in $Ca(OH)_2$ as the reference, the intensity ratios of physically bound water to $Ca(OH)_2$ were calculated for the 28 heating increments. Fig. 5 is the plot of these intensity ratios against heating increments. The curve shows diffusion-controlled characteristics and agrees well with those obtained by a gravimetric method. The data from both the NMR and gravimetric techniques are listed in Table I. While the physically bound water was driven out by heating, the chemically bound water and the "free" water trapped in the cement pores remained in the sample.

Depending on the size of the cement pores, the "free" water signal sometimes appeared as a Pake [24] doublet. When the size of the pores is small enough to restrict the free tumbling of the water molecules, molecular oscillation is the only motional alternative for the water. Thus, the two hydrogen atoms in H_2O are not equivalent and the dipolar coupling between the two protons gives $2I + 1 = 2$ peaks, in equal intensity, where I is the nuclear spin number. Fig. 6 shows the Pake doublet in the sample with a water-to-cement mass ratio of 0.4 which was obtained by an inversion-recovery multiple pulse sequence, π–τ–$\pi/2$.

After the physically adsorbed water had been driven out of the sample, the dried sample was soaked in distilled water for 10 min. During this period, water was physically absorbed back into the sample. The sample was removed and left to dry in air for 30 min. and then examined by NMR. Fig. 7, curves a, b and c, shows the spectra at 60 min, 80 min and 120 min, respectively, after the soaking. A large increase in the

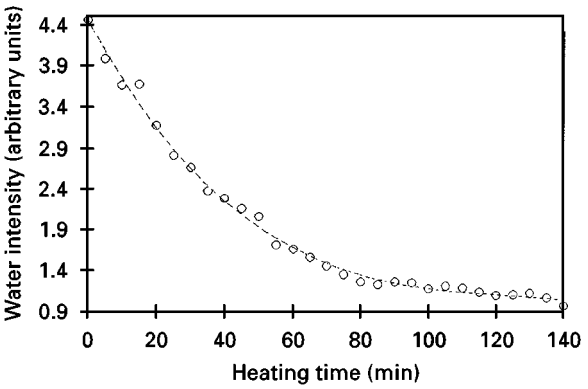

Figure 5 A plot of NMR intensity of physically bound water versus number of thermal treatments for the $w/c = 0.4$ sample, 33 days after mixing. The diffusion results agree very well with those from the gravimetric method shown in Fig. 3.

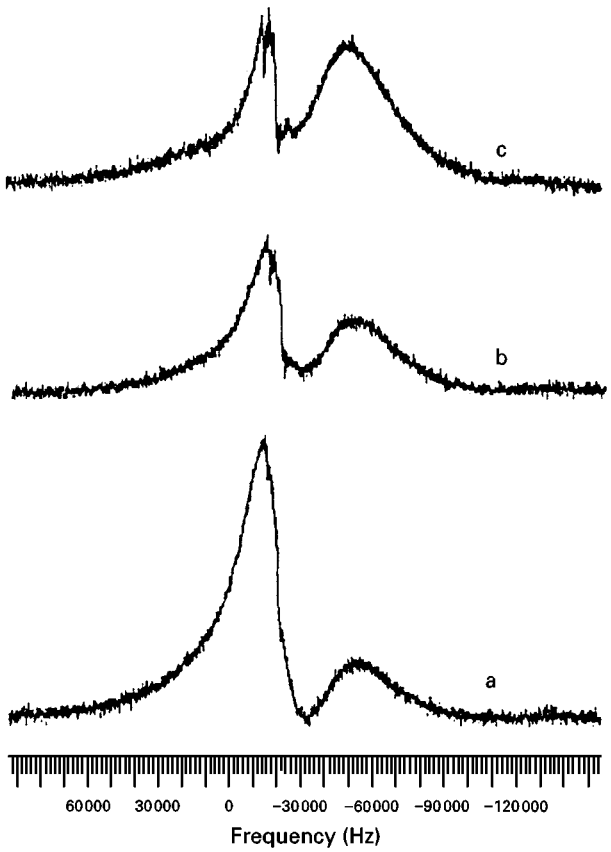

Figure 4 ^{1}H Fourier transform NMR spectra of a $w/c = 0.4$ sample after setting for 33 days. Curve a, before heating; curve b, ten treatments at 105 °C for 5 min each treatment; curve c, 20 treatments at 105 °C for 5 min each treatment. Physically bound water was removed in each treatment.

TABLE I ^{1}H NMR and gravimetric data of a 0.4 water-to-cement mass ratio sample setting for 33 days and heated at 105 °C for 5 min increments

Heating increment	Sample mass (g)	NMR intensity (arbitrary units)
0	0.6755	4.46
1	0.6649	3.99
2	0.6565	3.67
3	0.6493	3.68
4	0.6385	3.19
5	0.6303	2.82
6	0.6239	2.67
7	0.6178	2.38
8	0.6138	2.29
9	0.6097	2.16
10	0.6069	2.06
11	0.6006	1.71
12	0.5961	1.66
13	0.5920	1.56
14	0.5899	1.45
15	0.5867	1.41
16	0.5855	1.35
17	0.5840	1.26
18	0.5823	1.23
19	0.5806	1.26
20	0.5796	1.25
21	0.5784	1.18
22	0.5775	1.21
23	0.5769	1.19
24	0.5755	1.14
25	0.5744	1.10
26	0.5740	1.11
27	0.5730	1.13
28	0.5727	1.07

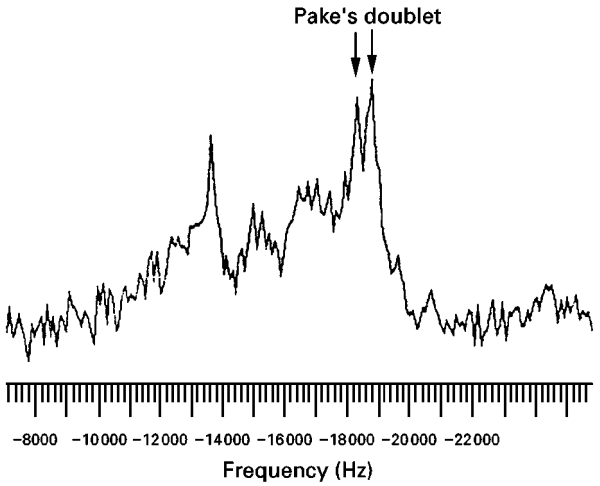

Figure 6 A Pake doublet was observed from a sample with pore size limiting the free rotation of water molecules. The spectrum was obtained by an inversion-recovery multiple-pulse sequence.

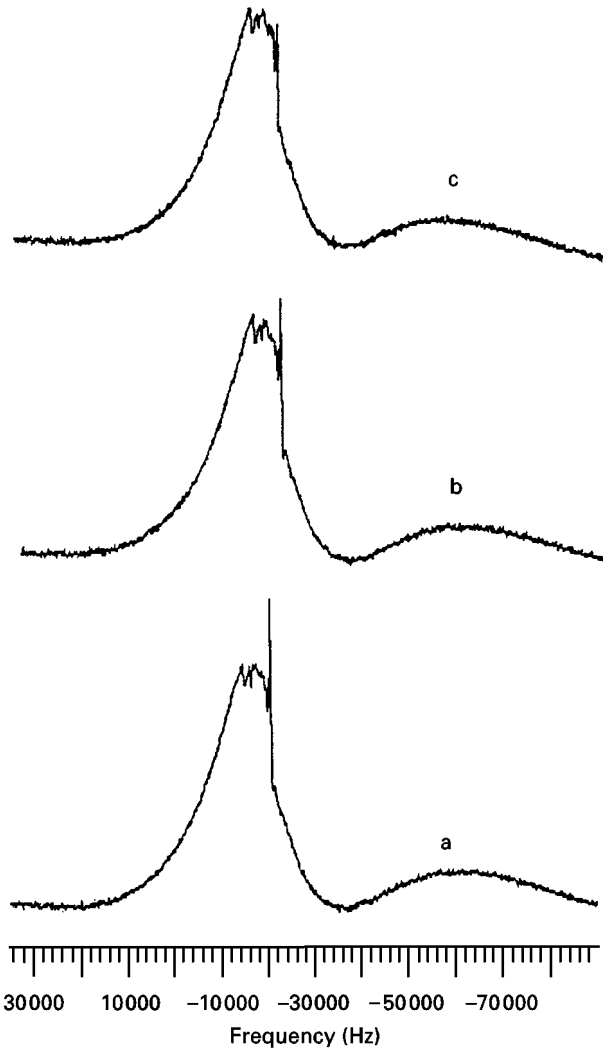

Figure 7 Spectra of a dry $w/c = 0.4$ sample soaked for 10 min in water and measured after 60 min (curve a), (b) 80 min (curve b) and 120 min (curve c) out of water, showing the diminishing free water.

intensity of the free water was observed. This suggests that the open pores or cracks in the cement were filled with water. However, this free water diminishes with time by either absorption or evaporation, because of

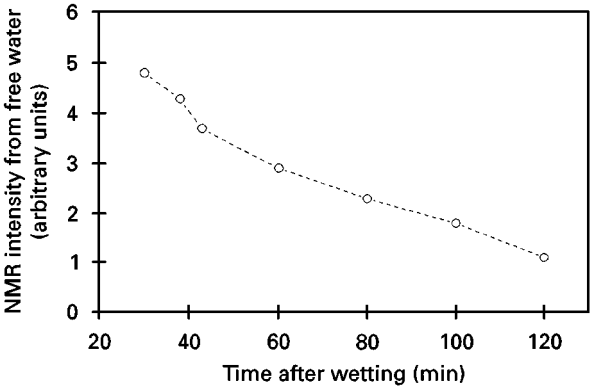

Figure 8 A plot of proton spin intensity of free water versus time standing in air after dipping a dry $w/c = 0.4$ sample in water for 10 min. The decay represents a combination of water diffusion and evaporation.

the open channels. A plot of free water intensities (again the ratio σ_1 to calcium hydroxide) is shown in Fig. 8. The proton spin intensity decay curve represents a combination of water diffusion and evaporation and appears to show a certain degree of linearity.

The relationship between the nuclear magnetization, M, and the magnetic field, H, are well described by Bloch's [25] equations. The nuclear spin–spin relaxation time, T_2, can be determined by measuring the spin echo intensity, I, observed at time, t, according to

$$I = I_0 \exp\left(-\frac{t}{T_2}\right) \quad (1)$$

where I_0 is the echo intensity at equillibrium using a pulse sequence of $\pi/2$–τ–π–τ and $t = 2\tau$ is a variable delay [26]. A set of τ values ranging from 0.15 to 40 ms with increments from 0.05 to 5 ms was used to perform the spin echo experiments for a sample with a 0.3 water-to-cement ratio 2 days after mixing. Echo signals were observed to decrease with increasing τ. Fig. 9 gives some examples of these echo signals at $\tau = 0.45$, 1, 4 and 35 ms. It is important to note that, when $\tau \approx 1$ ms, the echo signal changes both its decay rate and structure. When τ is smaller than 1 ms, the signal shows less "ringing" and decays more rapidly. This is an indication of a more rigid proton with a shorter T_2. These protons have been assigned to the physically bound water and a calculation using Equation 1 yields a T_2 value of 0.69 ± 0.01 ms. When τ is greater than 1 ms, the echo signal shows more ringing and decays more slowly. This is an indication of a more mobile proton. These protons are due to the chemically bound water with a –OH rotational narrowing of the $Ca(OH)_2$. A value of 85.90 ± 0.01 ms was obtained for the nuclear spin–spin relaxation time using Equation 1. The free tumbling water would also exist in this same region but was not observed since it was overwhelmed by the calcium hydroxide signal. The data are listed in Table II and a plot of the spin echo intensities against delay time is shown in Fig. 10. Two types of water can clearly be differentiated. The I_0 values in Equation 1 for the two types of water represent the relative number of spins for the chemically bound water and the physically bound water.

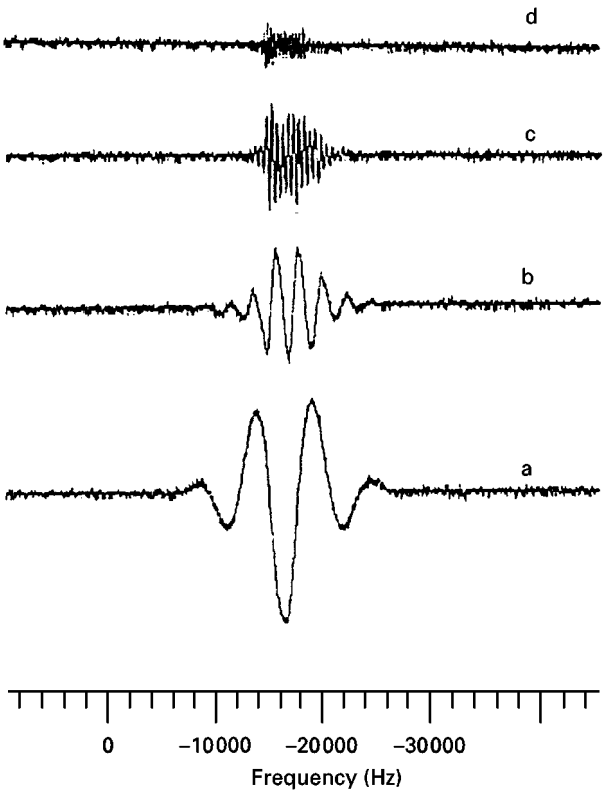

Figure 9 Nuclear spin-echo signals from a $w/c = 0.3$ sample (2 days setting) measured by spin echo at τ value of 0.45 ms (curve a), 1 ms (curve b), 4 ms (curve c) and 35 ms (curve d). When τ increases, both the intensity and the structure of the echo signal change.

TABLE II ^{1}H Spin-echo intensity decay at various delays for a 0.3 water-to-cement mass ratio

Delay τ (ms)	Nuclear spin-echo intensity (arbitrary units)	
	Experiment 1	Experiment 2 (2 h later)
0.15	60.0	58.0
0.20	56.0	54.0
0.25	49.0	47.0
0.30	43.0	41.0
0.35	36.0	37.0
0.40	31.5	33.0
0.45	26.5	27.5
0.50	24.0	25.0
0.55	21.5	22.5
0.60	19.5	21.5
0.65	18.0	20.5
0.70	17.5	19.0
0.75	16.0	18.5
0.90	13.5	15.0
1.00	13.0	14.5
4.00	12.0	14.3
8.00	10.3	13.0
10.00	10.0	12.5
13.00	10.0	11.0
15.00	8.5	11.0
17.00	7.5	10.0
20.00	6.8	6.3
23.00	6.4	7.8
25.00	5.8	6.8
27.00	5.1	6.5
30.00	4.0	5.5
35.00	3.9	4.5
40.00	1.9	2.0

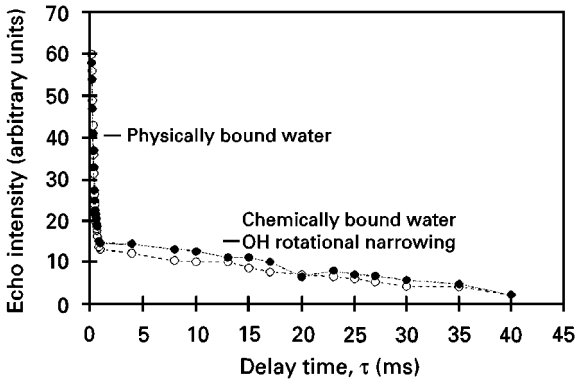

Figure 10 Nuclear spin-echo intensity decay curves of a $w/c = 0.3$ sample, measured 2 h apart. (○) , experiment 1; (●) , experiment 2 h later. Formation of $Ca(OH)_2$ can be detected.

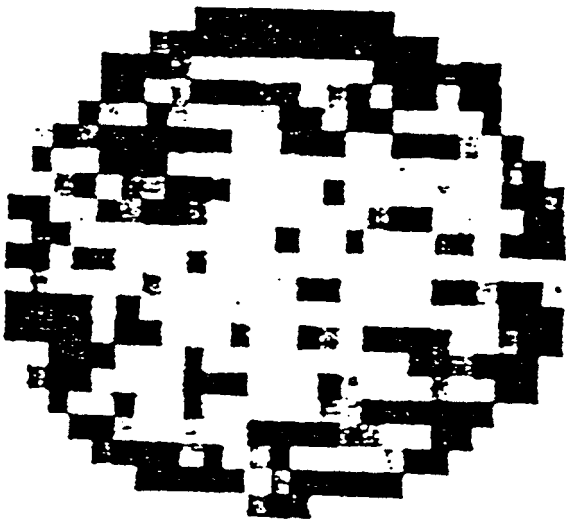

Figure 11 X–Y slice 34 of T_2-weighted proton imaging for solid mapping ($64 \times 64 \times 64$) of a dry $w/c = 0.3$ sample after soaking in water for 20 hs. The picture shows a doughnut shape, indicating only partial wetting. The picture size is 6 mm, from left to right.

The ratio of $(85.2 - 14.8) \pm 0.1$ was obtained for the physically and chemically bound water, respectively. Approximately 2 h later, the sample spin-echo experiments were repeated. The T_2 values were 0.66 ms and 78.5 ms and the relative intensities were 79.2 and 20.8 for the physically bound water and chemically bound water, respectively. Hydration reactions were detected during this 2 h period, thus making the cement harder and more $Ca(OH)_2$ rich. These data are also included in Table II and plotted in Fig. 10.

Finally, the 0.4 water-to-cement ratio paste sample was left in the oven to dry overnight at 105 °C. The "dry" sample was then studied again for moisture content. It was found, as expected, that all the physically bound water had been driven out. Only the chemically bound water, together with a trace of the "free" water trapped in the cement pores, remained. The dried sample was again soaked in distilled water overnight and re-examined for water absorption and diffusion. Both soft-pulse and hard-pulse techniques were used to image the water distribution inside the sample. With the soft-pulse technique, eight cross-sectional slices were taken while the sample was in the

water. The pictures showed a degree of distortion in intensity because of the artefacts from the ferrite materials. A 64 by 64 by 64 solid imaging experiment was performed while the sample was out of the water. Fig. 11 shows a slice on the X–Y plane. It shows only a ring along the cylindrical wall due to the water physically adsorbed during the overnight soaking. In the diffusion of water molecules, the initial diffusional motion is initiated by surface absorption and capillary effects of the porous material. However, because some air may have occupied the pores, the pressure of the air may reduce the diffusion rate and prevent water from wetting the core of the sample, even after overnight soaking [27]. However, leaving the sample in water for 3 days does wet the sample completely.

4. Conclusion

Three different types of water molecule, namely physically bound, chemically bound and porous-trapped or "free" water, were observed in hardened Portland cements by NMR. When the cement paste samples were heated at 105 °C, the physically bound water was driven out as a function of the heating time. The drying rate was found to be diffusion controlled. The chemically bound water remained in a stable calcium hydroxide form. The trace amount of "free" water was found to be encapsulated in the cement pores and showed a Pake doublet at times, depending on the size and distribution of the pores. Soaking the dried sample in water resulted in the diffusion of water back into the hardened cement in the physically bound state. The residual air occupying the pores is thought to reduce the diffusion rate. T_2-weighted imaging showed a doughnut shape for the distribution of the physically bound water after overnight soaking. A high water-to-cement ratio results in a heterogenous cement paste with a surface layer of $Ca(OH)_2$.

References

1. F. M. LEA, "The chemistry of cement and concrete" (Chemical Publishing Company, New York, 3rd Edn, 1971).
2. A. M. NEVILLE, "Properties of concrete" (Pitman Press, Bath, 1972).
3. D. P. BENTZ and E. J. GARBOCZI, *Cement Concr. Res.* **21** (1991) 325.
4. M. GEIKER, PhD thesis, Technical University of Denmark, Lyngby (1983).
5. H. F. W. TAYLOR, "Cement chemistry" (Academic Press, London, 1990).
6. P. COLOMBET and A. R. GRIMMER, "Application of NMR spectroscopy to cement science" (Gordon and Breach, New York, 1994).
7. G. PAPAVASSILIOU, F. MILIA, M. FARDIS, R. RUMM and E. LAGANAS, *J. Amer. Ceram. Soc.* **76** (1993) 2109.
8. J. C. MACTAVISH, L. MILJKOVIC, M. M. PINTAR, R. BLINC and G. LAHAJNAR, *Cement. Concr. Res.* **15** (1985) 367.
9. D. D. LASIC, M. M. PINTAR and R. BLINC, *Phil. Mag. Lett.* **58** (1988) 227.
10. S. BHATTACHARJA, M. MOUKWA, F. D'ORAZIO, J. YEHNG and W. P. HALPERIN, *Adv. Cement Based Mater.* **1** (1993) 67.
11. S. BHATTACHARJA, F. D'ORAZIO, J. C. TARCZON and W. P. HALPERIN, *J. Amer. Ceram. Soc.* **72** (1989) 2126.
12. F. D'ORAZIO, J. C. TARCZON, W. P. HALPERIN, K. EGUCHI and T. MIZUSAKI, *J. Appl. Phys.* **65** (1989) 742.
13. A. B. KUDRJAVTSEV, T. V. KOUZNETSOVA and A. V. PYATKOVA, *Cement. Concr. Res.* **20** (1990) 407.
14. T. V. KOUZNETSOVA and A. V. PYATKOVA, V. G. AKIMOV and A. B. KUDRJAVTSEV, *Trudy Musk. Khim.-Tekhnol. Inst.* **137** (1987) 101.
15. L. H. BENNETT, P. S. WANG and M. J. DONAHUE, *J. Appl. Phys.* **79** (1996) 4712.
16. P. S. WANG, D. B. MINOR and S. G. MALGHAN, *J. Mater. Sci.* **28** (1993) 4940.
17. P. S. WANG, S. G. MALGHAN, S. J. DAPKUNAS, K. F. HENS and R. RAMAN, *ibid.* **30** (1995) 1059.
18. *Idem., ibid.* **30** (1995) 1069.
19. P. S. WANG, *J. Mater. Sci.* (1996) submitted.
20. D. D. ELLMAN and D. WILLIAMS, *J. Chem. Phys.* **25** (1956) 742.
21. J. A. MORENO, S. MIZRACHI and V. OPPELTZ, *Solid State Commun.* **51** (1984) 597.
22. F. HOLUJ and J. WIECZOREK, *Can. J. Phys.* **55** (1977) 654.
23. D. M. HENDERSON and H. S. GUTOWSKY, *Am. Mineralogist* **47** (1962) 1231.
24. G. E. PAKE, *J. Chem. Phys.* **16** (1948) 327.
25. F. BLOCH, *Phys. Rev.* **70** (1946) 460.
26. C. P. SLICHTER, "Principles of magnetic resonance" (Springer, Berlin, 1989) Chapter 2.
27. P. S. WANG, (1998) to be published.

Received 28 May 1997
and accepted 18 March 1998